Earth Planet. Sci. Lett. 667 (2025) 119526

Contents lists available at ScienceDirect

Earth and Planetary Science Letters

journal homepage: www.elsevier.com/locate/epsl

# Phanerozoic orbital-scale glacio-eustatic variability

Douwe G. van der Meer [a,b,*], Lennert B. Stap [c,f], Christopher R. Scotese [d], Benjamin J.W. Mills [e], Appy Sluijs [b], Douwe J.J. van Hinsbergen [b]

[a] CNOOC International, ARC Building 3, Sanderson Rd, Uxbridge UB8 1DH, United Kingdom
[b] Department of Earth Sciences, Utrecht University, 3584 CB Utrecht, The Netherlands
[c] Now at: Statistics Netherlands, Henri Faasdreef 312, 2492 JP The Hague, The Netherlands
[d] Department of Earth and Planetary Sciences, Northwestern University, Evanston, IL 60208, USA
[e] School of Earth and Environment, University of Leeds, Leeds LS2 9JT, United Kingdom
[f] Institute for Marine and Atmospheric research Utrecht, Utrecht University, 3584 CC Utrecht, The Netherlands

ARTICLE INFO

Editor: Dr H Bao

ABSTRACT

Global Mean Sea Level, or eustasy, has a strong effect on depositional systems, biogeochemical cycles, and climate along continental margins. Long-term Phanerozoic Tectono-Glacio-Eustatic curves based on isotope geochemistry or plate reconstructions provide first-order trends but cannot resolve short-term (<1 Myr) high amplitude ice volume-forced variability, that resulted in glacio-eustatic fluctuations of >100 m during Paleozoic and Cenozoic icehouse times. These glacio-eustatic fluctuations were minor (~20 – 40 m) to absent during Mesozoic greenhouse climates. We provide a continuous quantification of maximum amplitude short-term sea level change during the last 540 million years. We utilize a high-resolution Cenozoic climate model to estimate orbital-scale ($10^3$-$10^5$ years) temperature and ice volume variations as a function of long-term (≥ 1 Myr) changes in ice volume. Building upon a recent long-term ice volume reconstruction, we then calculate maximum feasible orbital-scale cyclicity for the entire Phanerozoic. Our estimates of sea level change during greenhouse climates are much lower than some estimates based on stratigraphically derived eustatic reconstructions. This suggests that these stratigraphic methods overestimate orbital-scale sea level change or that these were caused by other factors such as aquifer eustasy. Our analysis quantifies the range of glacio-eustatic sea level variability that may be used as independent constraint in future paleoclimatologic, paleogeographic, paleontologic, and paleoceanographic research.

## 1. Introduction

Changes in the volume of ocean basins (tectonic eustasy) and in climate (glacio-eustasy) have caused fluctuations of global mean sea level (eustasy) by 100's of meters (Conrad, 2013; Haq and Cloetingh, 2025; Simmons et al., 2020; van der Meer et al., 2022) (Figure 1). Such sea level provides a first-order control on paleogeography, and thereby on paleoenvironment, paleoclimate, and paleobiology evolution as well as resource geology. However, quantifying sea level change comes with major challenges.

Classically, sea level variability is estimated from stratigraphic records contained in sedimentary basins (Vail et al., 1977; Sahagian et al., 1996; Browning et al., 1996; Haq and Al-Qahtani, 2005). However, regional geological influences on individual basin architecture and regional climate (Miall, 2010; Burgess and Prince, 2015) cannot be independently corrected for and most records come from proprietary seismic and well data that are not open to scrutiny by the scientific community (Miall, 2010; Burgess and Prince, 2015). Complimentary estimates from e.g., continental flooding (Scotese and Wright, 2018; Marcilly et al., 2022; Scotese et al., 2024) have a resolution of 1-10 Myr at best and datasets are incomplete due to erosion.

Recent research has therefore focused on long-term (>1 Myr) eustasy from plate tectonic reconstructions and proxies thereof (Karlsen et al., 2020; Spasojevic and Gurnis, 2012; van der Meer et al., 2017; Vérard et al., 2015; Wright et al., 2020; Young et al., 2022), glacio-eustasy from reconstructed ice areas (Scotese et al., 2024, 2021; Scotese and Wright, 2018) (Figure 1), and ice volumes (van der Meer et al., 2022). These resulted in an estimated glacio-eustatic sea level curve in 1 Myr time steps, which included an uncertainty stemming from underlying assumptions (van der Meer et al., 2022). However, these curves so far

* Corresponding authors.
*E-mail address:* Douwe.vanderMeer@intl.cnoocltd.com (D.G. van der Meer).

https://doi.org/10.1016/j.epsl.2025.119526
Received 15 April 2025; Received in revised form 20 June 2025; Accepted 23 June 2025

overlooked the effect of orbital-forced (Milankovitch-cycle) changes that are well-known from the sedimentary records for the last billion years (De Vleeschouwer et al., 2024; Hinnov, 2013; Kent et al., 2018; Mitchell et al., 2021). The Milankovitch cycles may cause eustatic sea level changes at much higher frequency and are dominated by precession (~20 kyr), obliquity (~41 kyr), and eccentricity (~100 and ~400 kyr) (Laskar, 2020; Milanković, 1930). This is particularly significant in ice-house worlds (Stap et al., 2017; Rohling et al., 2022; Miller et al., 2024) and the amplitude of orbital-scale, short term (<1 Myr) Cenozoic eustasy (Stap et al., 2017) exceeds the estimated errors of long-term (>1 Myr) eustasy (van der Meer et al., 2022), which represent the best-estimate averages over 1 million year time steps.

Phanerozoic global mean sea level curves, so far, have not taken this short-term orbital-scale variability into account even though much of the geological record is produced by short-term climate and sea level extremes rather than long-term averages (Alley et al., 2020; Boucot et al., 2013; Davies and Simmons, 2024; Scotese et al., 2021). The overall amplitude of orbital-scale eustatic cyclicity during the Phanerozoic is thus a crucial but lacking parameter (Davies and Simmons, 2024). Here, we aim to arrive at the first-ever retrodiction of short-term orbital-scale glacio-eustasy for the past 540 million years, by combining the recent estimate of Phanerozoic long-term ice volume (van der Meer et al., 2022) with the orbital-scale variability deduced from well-constrained Cenozoic land ice models (Stap et al., 2017). Therefore, we first derive a relationship between short-term, orbital-scale glacio-eustatic variability and long-term ice volumes (Figure 2) and then add the (maximum) short-term variability in global mean sea level due to Milankovitch cyclicity to the long-term average, as an indirect estimate of the uncertainty in long-term eustatic curves.

### 1.1. *Orbital-scale temperature and ice volume changes produced by Milankovitch cyclicity*

Several recent studies have estimated the Earth's changing temperature during the Phanerozoic based on lithologic indicators of climate, geochemical proxies such as oxygen isotopes, and computer simulations

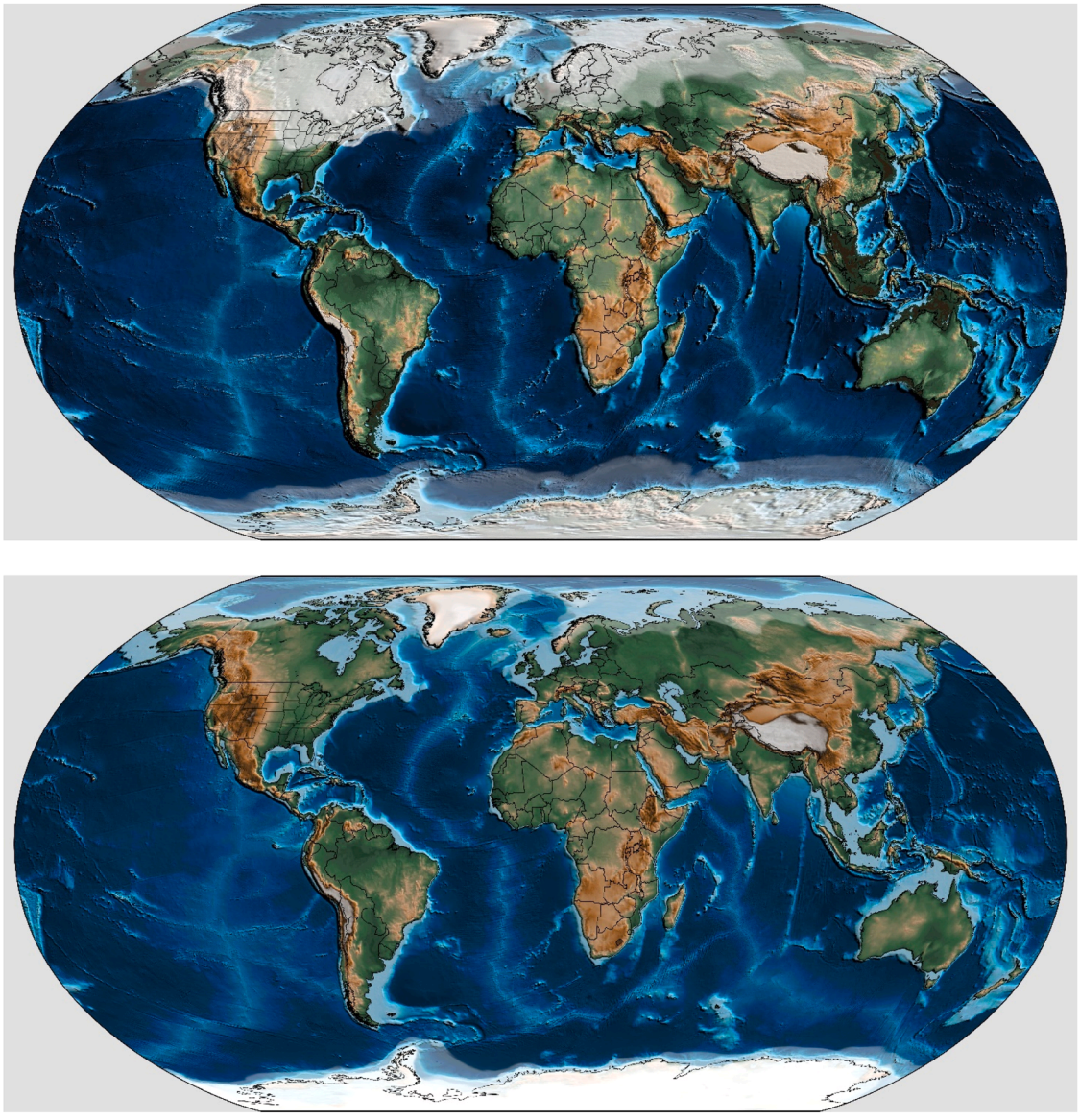

**Fig. 1. Paleogeographic reconstructions** (Scotese et al., 2024; Scotese and Wright, 2018). **A)** Last Glacial Maximum (~20 ka), an example of maximum glacial extent, low global mean sea level and more exposed continental shelf. As a result of changing continental ice-cover, glacio-eustasy results in changes in eustasy and flooding of continents. **B)** Present-Day, as example of an Interglacial with relatively high sea level. Long-term sea level reconstructions do not consider short-term changes in sea level due to orbital-scale variations.

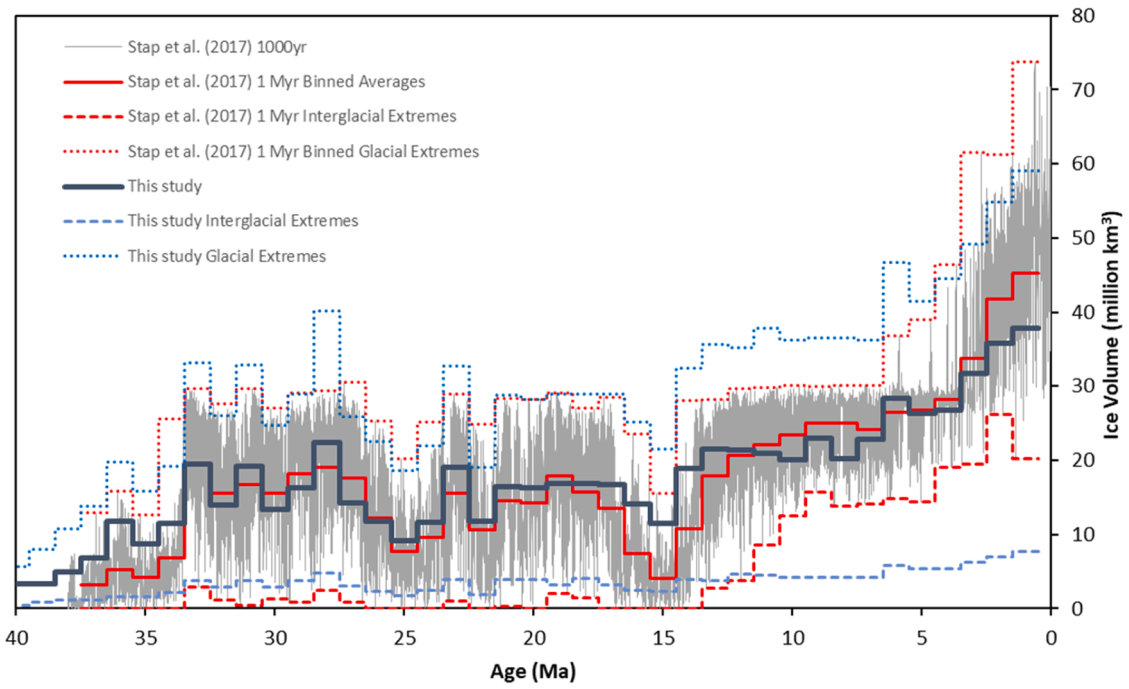


**Fig. 2. Calibration of ice volumes during the Cenozoic**. A 1-dimensional Cenozoic climate model (Stap et al., 2017) produces orbital-scale ice volume variability at 1000 year steps (grey lines), which were combined into one million year averages, maxima and minima (red bold and dotted lines). Our spatial ice area ($km^2$) reconstruction (blue bold and dotted lines), was calibrated between 37-6 Ma with the ice volumes ($km^3$) of the Cenozoic climate model (Stap et al., 2017) yielding best-fit ice thicknesses for the average (1334 m), minimum (491 m) and maximum (1542 m) scenarios respectively. Assuming that these ice thicknesses remained constant during the Phanerozoic, this allowed a first-order approximation of orbital-scale ice-volume variability based on our long-term ice reconstruction (van der Meer et al., 2022) which was constructed using the paleotemperature model of Scotese et al. (2021).

of past climate (Mills et al., 2019; Scotese et al., 2021; Valdes et al., 2021; Judd et al., 2024). However, these estimates of Phanerozoic temperatures (Figures 2, 3) do not take into account orbital variability at <1 Myr. Climate feedback mechanisms are also poorly constrained in these studies.

By measuring the ratio of $^{18}O$ to $^{16}O$ in carbonate or apatite microfossils, also typically reported as $\delta^{18}O$, it is possible to estimate the temperature (Scotese et al., 2021) at which the calcium carbonate or apatite was produced. For the Cenozoic, however, Stap et al. (2017) used a combined physical global ice-sheet-climate model to deconvolve stacked high-resolution deep ocean benthic foraminifer $\delta^{18}O$ data (Zachos et al., 2008). Their relatively simple 1D ice sheet model was combined with a zonally averaged energy balance climate model, to simulate mutually agreeing records of $CO_2$, meridional paleotemperature, and ice volume (sea level) over the past 38 Myr, at 1000-year resolution.

The error estimates of long-term global average temperature (Scotese et al., 2021) for the Cenozoic, are generally within the variability of the orbital-scale reconstruction (Stap et al., 2017) (Figures 2,3). The long-term temperature errors were estimated by van der Meer et al., (2022) by calculating the Root-Mean-Square error of the Köppen-zone uncertainty range, which was based on the number of sample localities (Boucot et al., 2013; Scotese et al., 2021), with the Phanerozoic temperature reconstruction derived from $\delta^{18}O$ data (Song et al., 2019). The latter inherently included scatter of the $\delta^{18}O$ data due to orbital-scale cyclicity, which is the variability in the long-term trend that we aim to identify here.

### *1.2. Long-term temperature and ice volume as a proxy for short-term orbital scale glacial variability*

The various approaches that use oxygen isotopes, ice volume and deep ocean temperature to predict polar temperatures (Miller et al., 2024; Rohling et al., 2022; Stap et al., 2017), indicate that short-term orbital-scale ice variability increases as a function of long-term ice volume (Figure 3). Notably in the Pleistocene global land ice volumes and temperature fluctuations have been the largest, but when there is no long-term ice (i.e. Eocene), there is generally no short-term orbital-scale variation in ice volume. From these observations, we infer that large long-term volumes of continental ice are associated with large swings in temperature due to orbital periodicities. The larger amplitude in ice volume was driven by a stronger ice sheet height-mass balance feedback, and stronger global ice-albedo positive feedback as ice fronts reached lower latitudes during glacial times. This glacial/interglacial cycle is driven by stronger positive carbon cycle feedbacks (Intergovernmental Panel on Climate Change (IPCC), 2023; Rohling et al., 2012).

The temperature variability from the mean at 1 Myr binned time steps of the 1-D climate model (Stap et al., 2017) are on average ±0.9 °C between 37-1 Ma (Figure 4). This temperature variability increases throughout the Cenozoic as result of lowering global average temperature, and hence there were more extensive continental ice sheets. In our Cenozoic climate model (Stap et al., 2017) the temperature variability is ±2.5 °C at one million years. However, this short-term variability could still be an underestimate, as other studies of Pleistocene temperatures suggest that short-term temperature variability could have been as high as ±3.5 °C during the last 800 ka (Köhler et al., 2018) and as high as ±4.5 °C during the last 23 ka (Osman et al., 2021).

During the (functionally) ice-free late Eocene, there was large orbital-scale deep ocean temperature variability on the order of ±1 °C based on foraminifer $\delta^{18}O$ data (Westerhold et al., 2020). Recent research has also quantified eccentricity-forced global mean sea surface temperature variability during the ice-free early Eocene at ~±1 °C as well (Fokkema et al., 2024). Along with carbon cycle and ice-related climate feedbacks, another reason for larger temperature swings in the late Cenozoic is the non-linear relationship between $CO_2$ and temperature, which makes low-$CO_2$ climates (i.e. late Cenozoic) more sensitive to a given absolute $CO_2$ change than at high $CO_2$ (i.e. early Eocene) (Intergovernmental Panel on Climate Change (IPCC), 2023).

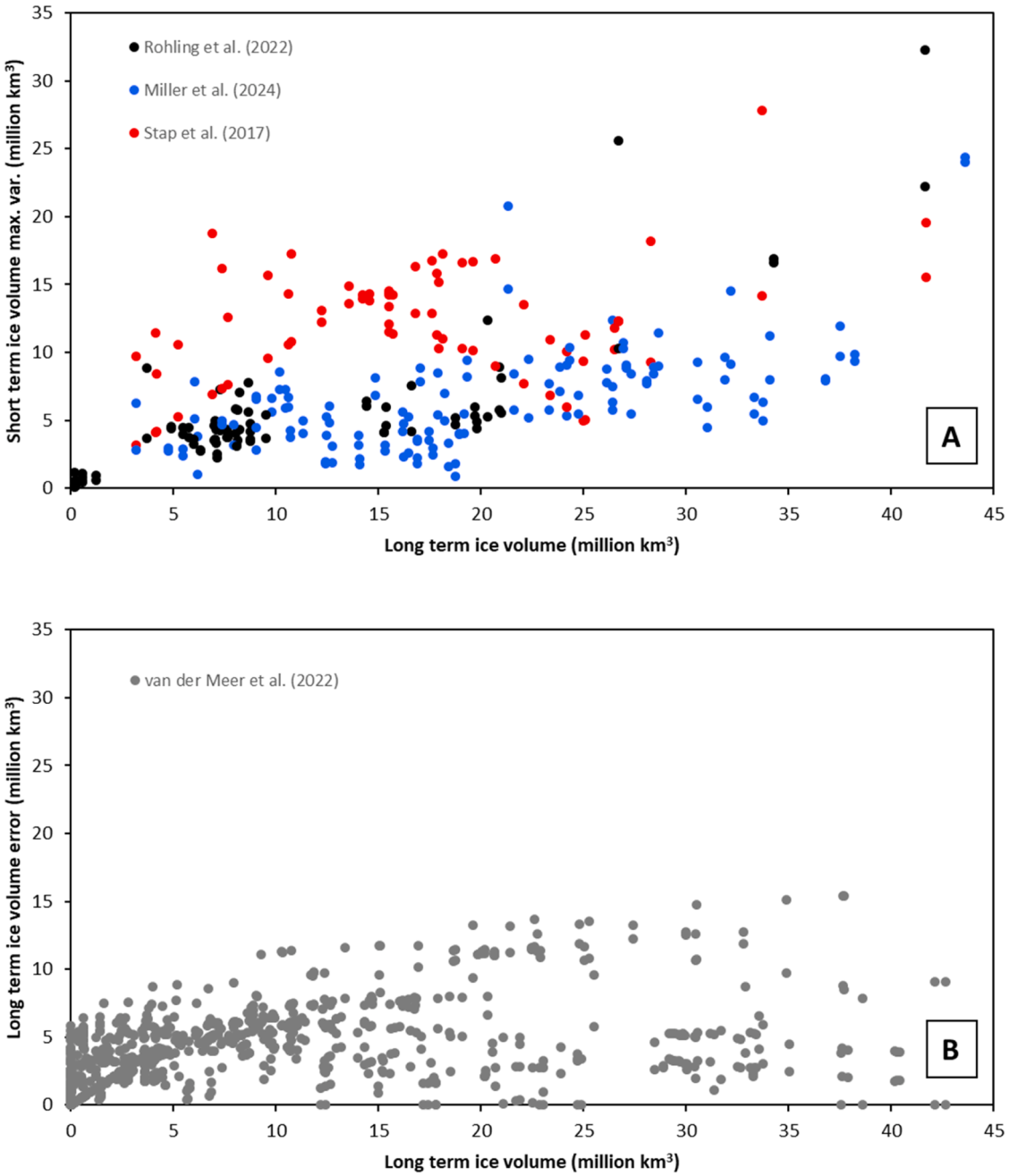


**Fig. 3. Short-term ice volume variability as a function of long-term ice volume. A)** Ice volume maximum variability of 3 climate models (Miller et al., 2024; Rohling et al., 2022; Stap et al., 2017). Due to positive feedback mechanisms related to ice-albedo effect, the variability of the short-term ice volume generally increases with increasing long-term ice volume. This is known as the "polar amplification" effect (Valdes et al., 2021). Simply stated, the larger the area of the (long-term) polar ice cap, the greater the amplitude of short-term changes polar ice sheets areas. Dots represent the variations from the mean ice volume due to (extreme) glacial and interglacial periods, binned every 1 Myr. In comparison these are at least just as significant as **B)** error estimates of long-term ice volume reconstruction (van der Meer et al., 2022), based on the paleotemperature model of Scotese et al. (2021) from which temperature and paleo-Köppen-zone uncertainties were propagated.

Reconstructed long-term ice volumes as calculated by Van der Meer et al. (2022) require land at high latitudes (Scotese and Wright, 2018), and global average surface temperature less than 18 °C (Scotese et al., 2021). At that average global temperature, there are paleolatitudes close to the pole where the annual average temperature is less than -10 °C which is the temperature required to maintain snow and ice cover, year-round (van der Meer et al., 2022). Following the methodology of Mills et al., (2019), van der Meer et al. (2022) estimated the paleo-latitudes of perennial ice, by using the linear relationship between Cenozoic global average temperatures and the paleo-latitudes of the -10 °C isotherm. Using the global average temperatures of Scotese et al. (2021), combined with the distribution of land and continental shelf (Scotese and Wright, 2018), ice areas and volumes were calculated at 1 Myr steps between 540-0 Ma (van der Meer et al., 2022).

### *1.3. Long-term icehouse conditions leading to orbital-scale temperature and ice variability*

We infer a polynomial relationship between long-term ice volumes and orbital-scale temperature variability (Figure 4). Using the Cenozoic

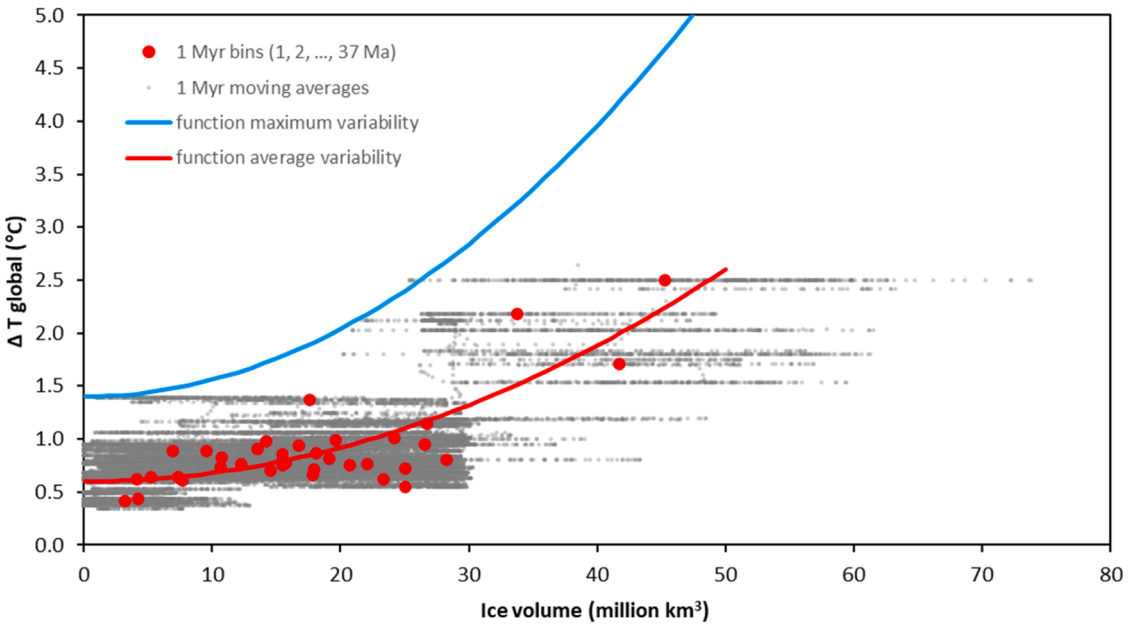


**Fig. 4. Ice sheet volume versus temperature variability during the Cenozoic.** Temperature variability from the mean, as a function of long-term ice volumes. Red dots represent 1 Myr averages of every 1 Ma step between 1-37 Ma of the climate model (Stap et al., 2017). Grey dots are 1 Myr moving averages of the 1 kyr model outputs. Red line: average variability function. Light blue line: maximum expected temperature variability that fits most of the Cenozoic 1-D climate model (Stap et al., 2017). Note the large step in the temperature variability when the ice volume reaches 30 million km$^3$ which is due to the geographical limitations of the Antarctic and Northern hemisphere ice sheets.

1-D climate model (Stap et al., 2017), and averaged over 1 Myr, we infer a maximum orbital-scale temperature variability ($\Delta T$) as a function of long-term mean ice volume (see Materials and Methods, Supplementary Information). The spread in Cenozoic datapoints is the result of the land (ice) configuration which is non-continuous. There is a divide at ~30 million km$^3$ , leading to a 'step' in data points, that is caused by the geometrically limited distributions of the Antarctica and the Northern Hemisphere ice sheets (De Boer et al., 2010; Stap et al., 2017). If there would have been a more equal distribution of continents globally in the Cenozoic (i.e. at southern latitudes north of Antarctica), a more even spread of (grey) datapoints would be expected. In addition to changing land distribution, there is a strong hysteresis in the dynamics of ice sheets, whereby ice sheets tend to jump in size because of their non-linear response to climate change. Nevertheless, the maximum

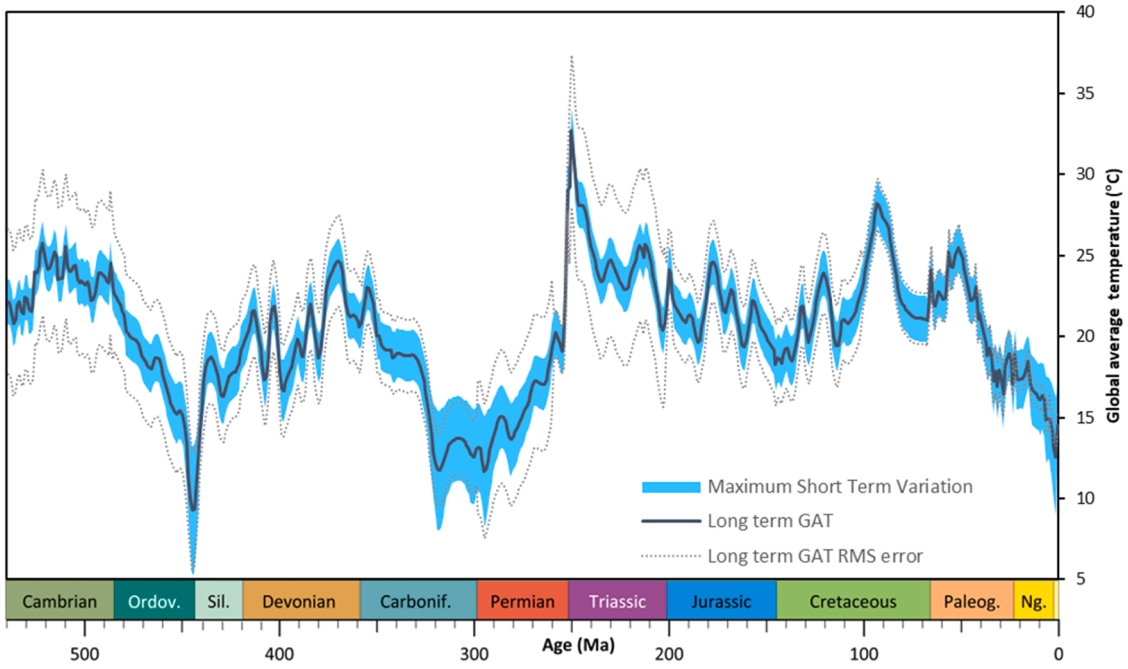


**Fig. 5. Phanerozoic Paleotemperature variability.** Estimated orbital-scale temperature variability from the mean long-term Global Average Temperature (GAT) of Scotese et al. (2021) for 540-6 Ma, and Stap et al. (2017) for 5-1 Ma. Note the larger variability during the icehouse climates of the late Cenozoic, Permo-Carboniferous, and late Ordovician versus smaller variability during intervening greenhouse climates. During the Neogene and Permo-Carboniferous, orbital-scale variability is larger than, or equivalent to, the long-term RMS errors (grey dotted lines) (van der Meer et al., 2022).

possible temperature variability (blue curve, Figure 2) we define here, can be applied to any other time, as we consider different land configurations throughout the Phanerozoic later in our calculations.

Using the maximum feasible temperature variability between (extreme) glacial and interglacial periods, we subsequently derive minimum and maximum ice volumes over the Phanerozoic and hence the extremes of orbital-scale glacio-eustasy. This is subsequently tested with glacial deposits in the geological record, and orbital-scale glacio-eustasy estimates from the literature.

We used the short-term variation in global temperature (Figure 5) to estimate the range of global temperatures for any specific time interval. For example, during the depths of the Permo-Carboniferous Ice Age (~300 Ma), global average temperatures may have ranged from 17 °C during the warmest interglacial to 10 °C during the coldest glacial epoch. Using these variations in temperature we estimated the perennial ice front following our earlier approach (van der Meer et al., 2022) (Materials and Methods, Supplementary Figure 1). In the next step we calculated ice areas and ice volumes that covered land areas and the continental shelf at high latitudes using the digital model of paleo-elevation (Scotese and Wright, 2018) (Supplementary Figures 2 and 3). A best-fit ice thickness (1334 m) for the Cenozoic was obtained by calibrating long-term ice areas (van der Meer et al., 2022), with late Cenozoic ice volumes (1 Myr averages) of the more detailed climate model estimates (Stap et al., 2017) (Figure 2). In other words, we assumed that the relationship between ice area and ice volume that has been established for the Cenozoic, can be subsequently applied to estimate the size of ice caps of other icehouse periods throughout the Phanerozoic (Supplementary Figure 3).

From ice-volumes (Supplementary Figure 3) we calculate the range of orbital-scale glacio-eustasy using the methodology for long-term eustasy described in (van der Meer et al., 2022). However, there is one key difference. Whereas long-term (≥1 Myr) glacio-eustasy was assumed to be isostatically compensated, in this study it was assumed the maximum orbital-scale variability (i.e. 1000-year scale), is too rapid for a complete isostatic rebound. Without accounting for isostatic rebound compensation, orbital-scale sea levels may have temporarily exceeded global mean sea level due to the melting of the ice that remained in the long-term ice cover reconstruction (Supplementary Figure 4). Overall, we estimate that melting the present-day ice covering Antarctica and Greenland would lead to a ~57 m sea level rise, if isostatically compensated. During an extreme interglacial interval global mean sea level could have risen as much as ~68 m, if rising seas were not isostatically compensated. This is in general agreement with other published estimates (Clark et al., 2016).

We combine the orbital-scale glacio-eustatic reconstruction derived here with the long-term Tectono-Glacio-Eustatic curve (van der Meer et al., 2022) to illustrate our estimate of Global Mean Sea Level variability during the last 540 million years (Figure 6). During the late Ordovician, Permo-Carboniferous, and late Cenozoic icehouses, our estimate of maximum orbital-scale glacio-eustatic variability is very large (>100 m). This is similar to the first-order long-term eustatic variability that is of predominantly tectonic origin. During the middle Ordovician to early Carboniferous (460 Ma – 340 Ma), and Late Jurassic to early Cretaceous (160 Ma – 110 Ma), we predict that limited amounts of glacio-eustasy (10's of meters) occurred, like 2$^{nd}$ order long-term tectono-glacio-eustatic cycles. During the Cambrian to early Ordovician (540 Ma – 470 Ma), the Triassic to middle Jurassic (250 Ma – 160 Ma), the mid-Cretaceous (100 Ma – 80 Ma), and the early Eocene (55 Ma – 40 Ma) very limited orbital-scale glacio-eustasy occurred, due to the very limited presence of (long-term) continental ice. Periods that exhibit only orbital-scale glacio-eustatic episodes do occur, but they are rare and of very short duration (less than a few million years).

## 2. Discussion

This paper represents the first attempt to calculate sea level changes during the Phanerozoic at temporal resolution of thousands to 100's of thousands of years using first order principles. Eustasy is estimated using global changes in temperature (Scotese et al., 2021) and the consequent changes in the size of the polar icecaps combined with long-term sea level change which is ultimately due to the changing volume of the ocean basins and the hypsometry of the continents (Van der Meer et al., 2022).

In this section of the paper, we test our estimates of paleolatitudes of perennial ice formation with the Phanerozoic record of glacial deposits (Alley et al., 2020; Scotese et al., 2021). Indeed, calculated

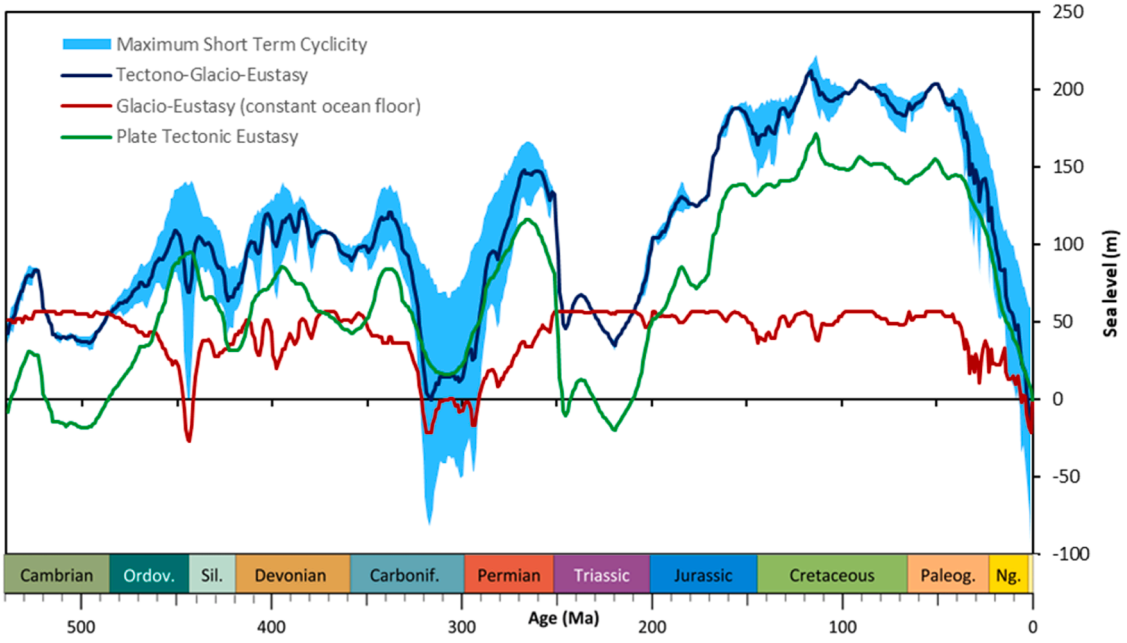


**Fig. 6. Global Mean Sea Level curve with maximum and minimum sea level excursions.** Isostatically compensated effects of long-term plate tectonics (green line) and ice (red line), are combined in the Tectono-Glacio-Eustatic curve (dark blue line). The light blue shading illustrates the maximum range of short-term sea level cyclicity.

paleo-latitudes of the perennial ice orbital-scale cyclicity extremes are closer to the lowest latitudes of recorded glacial deposits than the long-term average, during the 3 major Phanerozoic icehouse periods (Late Cenozoic, Permo-Carboniferous and Ordovician-Silurian; supplementary Figure 1). Hence, we conclude that our calculations correspond well to the geological record of ice sheet paleogeography to first order. However, we note discrepancies for periods for which no glacial deposits have been documented (Alley et al., 2020; Scotese et al., 2021). These may have several causes. First, Scotese et al. (2021) have plotted the extreme (lowest latitude) occurrences of glacial evidence, whereas the average paleo-latitude of the ice front would have been at a somewhat higher latitude. Second, there may be incompleteness of data at high latitudes due to inaccessibility or reduced preservation. Third, the relationship between paleo-latitude of the ice front and global mean temperature was simplified and represented as a linear function (van der Meer et al., 2022), following the approach of preceding studies (Mills et al., 2019). A non-linear function may be defined, including asymmetry between the hemispheres as suggested in pole-to-equator temperature gradient diagrams (Scotese et al., 2024, 2021). Overall it should be noted that there is still debate on Phanerozoic paleotemperature estimates (Judd et al., 2024; Mills et al., 2019; Scotese et al., 2021; Valdes et al., 2021). Even for the Cenozoic, considerable differences exist between climate models (i.e. temperature, ice extents and variability) (Miller et al., 2024; Rohling et al., 2022; Stap et al., 2017). A recent model of Phanerozoic temperatures based on proxy data assimilation into coupled ocean atmosphere climate model simulations (Judd et al., 2024) proposes that global temperatures were extremely warm, i.e. 8-12 °C warmer than other global temperature models (Grossman and Joachimski, 2022; Scotese et al., 2021; Valdes et al., 2021). Judd et al. (2024) calculate extremely high temperatures during (parts of) the Ordovician-Devonian, Cretaceous, and early Cenozoic, which would exceed the lethal limit for marine life (>30 °C global average temperature). For our analyses in particular, these proposed high temperatures would have prohibited the formation of large (>5 million km$^2$), long-term, polar ice caps during the early Paleozoic, Mesozoic and most of the Cenozoic (until 10 Ma), which would be in conflict with lithological paleo-climate indicators (i.e. tillites, dropstones and glendonites) (Alley et al., 2020; Boucot et al., 2013; Scotese et al., 2021), such as the start of Antarctic glaciation starting at least 20 million years earlier (Barker et al., 2007) than what would follow from the Judd et al. reconstruction. This aberration requires a correction of the $\delta^{18}O$ derived temperature curve, such as performed by several studies (Prokoph et al., 2008; Scotese et al., 2021; Shaviv et al., 2023). For this reason, this model (Judd et al., 2024) was not considered in this study. We expect that further refinements to the estimates of long-term and orbital-scale ice variability will be possible in the future through paleo-ice sheet modelling (i.e. Kirchner et al., 2011).

The contrasting amounts of (maximum possible) orbital-scale glacio-eustasy during the Phanerozoic (Figure 7), can be tested with sedimentological records. This curve also provides a means to distinguish global forcing of sequence-stratigraphy and other, local or autogenic drivers. Because eustatic variations within a single sedimentary basin is usually not representative of global mean sea level fluctuations, we prefer to compare eustasy between several basins covering the same time interval which provides means of stratigraphic verification. Especially useful are the quantifications derived in compilation studies for the Silurian (Johnson, 2010), Permo-Carboniferous (Rygel et al., 2008) and Cretaceous (Ray et al., 2019). Additional literature only provides indications of glacio-eustatic cyclicity, but these are generally hampered by limited number of studied sedimentary basins, or lack of quantification. Chronologically, the evidence for short-term glacio-eustasy is as follows.

For the Cambrian, Babcock et al. (2015) concluded that this period was a generally warm interval of relatively high sea level, but it was punctuated by brief episodes of change, of which the abruptness and synchroneity of sea level change strongly implied glacio-eustasy. This is consistent with our reconstruction whereby we infer the possibility of limited (<15 m) short-term glacio-eustatic cyclicity.

For the Silurian, Johnson (2010) compiled eustatic changes for the Silurian across five paleo-continents (Laurentia, Avalonia, Baltica, Bohemia, and Gondwana). The best documented Silurian sea level rises are documented by burial of coastal topography in the early Silurian and were up to 70 m (Johnson et al., 1998). These provided estimates enabled us to quantify the (maximum) change over 1 Myr intervals of the Johnson (2010) indicative eustatic curve.

Additionally, some literature data for the Ordovician-Silurian is

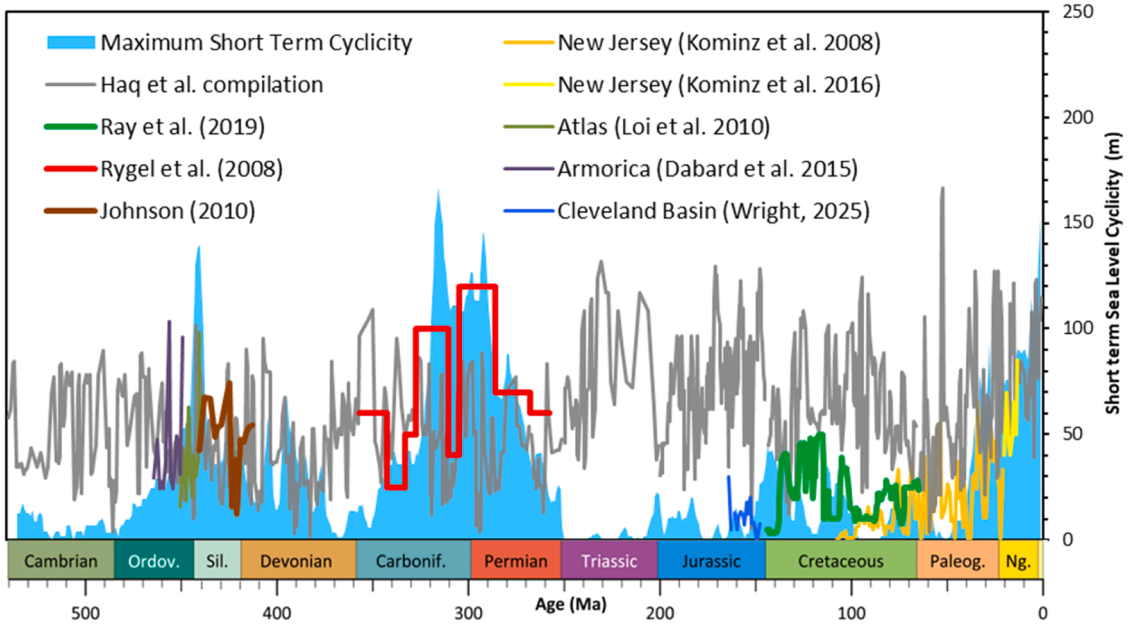


**Fig. 7. Orbital-scale glacio-eustatic cyclicity.** Our estimate of the maximum cyclicity (light blue polygon) and comparison with maximum short-term estimates in compilations (bold lines) from the global sedimentary record (Johnson, 2010; Ray et al., 2019; Rygel et al., 2008), individual basins (thin lines) (Dabard et al., 2015; Kominz et al., 2016, 2008; Loi et al., 2010), and stratigraphic estimates of Haq et al. (Haq and Ogg, 2024; Haq, 2018a, 2018b, 2014; Haq and Schutter, 2008) (grey line).

available that quantified orbital-scale glacio-eustasy in the Atlas Mountains (Loi et al., 2010), and Armorica (Dabard et al., 2015), by back-stripping the basins' stratigraphy. Although the (regional) relative sea level variability as calculated in these studies are not necessarily representing (global) eustasy, we do note that there is no major discrepancy with our orbital-scale cyclicity estimates which were large in the Ordovician-Silurian.

For the Devonian (Johnson et al., 1985) correlated synchronous events in 5 regions in North America and Europe. At least 14 transgressive-regressive cycles are recognised of which the synchroneity indicates control by eustatic sea-level fluctuations. These fluctuations are however not quantified. More recently (Elrick et al., 2009) based on stratigraphic sections in Europe and North America and $\delta^{18}O$ analyses, concluded that glacio-eustatic sea-level changes of >35 m would have occurred in the early-middle Devonian at 1 Myr time scales. Whereas at <100 kyr timescales in the Middle Devonian, ~15-23 m glacio-eustatic oscillations were estimated. These estimates are in agreement with our estimates of a maximum of up to 70 m short term cyclicity in this interval (but generally less).

Rygel et al. (2008) incorporated results from over 100 publications to summarize late Paleozoic orbital-scale glacio-eustatic cycles. They concluded that glacio-eustatic fluctuations of up to 120 m occurred between the late Carboniferous to early Permian. Since the publication of Rygel et al. (2008), glacio-eustatic cycles have been corroborated in more recent studies on individual basins, with amplitudes ranging from tens of meters during the middle Carboniferous as estimated for the Dniepr-Donets Basin (van Hinsbergen et al., 2015) to 100 meters during the early Permian in the Carnic Alps (Austria) and Robledo Mountains (New Mexico, USA) (Calvo González et al., 2022), the latter being contemporaneous with the acme of the main phase of the Late Paleozoic icehouse. These magnitudes are comparable to our estimates of eustasy during the same interval.

In the Triassic no published literature is available regarding long or short term glacio-eustasy, in agreement with our reconstruction. In contrary, due to the absence of glacio-eustasy, aquifer-eustasy has been documented to have been a possible dominant eustatic factor (Davies et al., 2020; Wagreich et al., 2014).

For the Jurassic, glacio-eustatic cycles have been inferred throughout the Jurassic in the Adriatic carbonate platform (Husinec et al., 2022), but these have not been quantified. Only in the Cleveland Basin, relative short term sea level variation was recently quantified to be up to 30 m, but generally less than 20 m (Wright, 2025).

Ray et al. (2019) compiled 160 stratigraphic studies covering the entire Cretaceous. Of these, approximately 50% describe the absolute magnitude sea level change. The remaining 50% provide unique stratigraphic records that clearly document the methodology and sea level interpretations for each study area. Except for the late Albian to Turonian hothouse (~110-90 Ma), where sea level fluctuations were <10 m, they concluded that orbital-scale sea level in the Cretaceous varied by up to 50 m. This agrees with the sea level variability proposed by our study.

For the Cenozoic there is no similar compilation based on the stratigraphic record. Glacio-eustasy is generally thought to have started either in the later Eocene and is not disputed since the Oligocene. Our results favourably compare with a high-resolution relative sea-level reconstruction from New Jersey (Kominz et al., 2016, 2008) (see Figure 7).

Overall, the eustatic signatures of these studies are modest (<20 m) to moderate (<60 m) during greenhouse intervals and exhibit large amplitudes (~100 m) of sea level change during the Ordovician-Silurian, Permo-Carboniferous and mid-late Cenozoic icehouse periods (Figure 7). These studies, derived mostly from stratigraphic information, corroborate our estimates of eustasy that are based on first-order principles. Our estimates of orbital-scale cyclicity are derived from oxygen isotope geochemistry, the changing land configurations and utilize a Cenozoic climate model as a reference frame for icehouse worlds.

We also compare our eustatic curve to a compilation of the most recent eustatic curves of Haq et al. (Haq and Ogg, 2024; Haq, 2018a, 2018b, 2014; Haq and Schutter, 2008). These studies, based on sequence stratigraphy, are the most recent estimates of global mean sea level variability during the Phanerozoic based on sequence stratigraphy. It should be noted that Haq et al.'s sea level curves are based on the onlap and offlap of sedimentary sequences that have been corrected for sediment loading and compaction. These estimates of eustatic change are based on well-correlated, seismically calibrated regional stratigraphic sequences along a variety of passive margins. The absolute magnitude of these seismically calibrated eustatic events, however, is difficult to quantify. The peaks and troughs in Haq's curves are typically spaced every 0.5 to a few million years apart, and therefore have much lower resolution than our estimates of (maximum) orbital-scale eustatic variability. Most notable is the fact that the maximum amplitude of the sea level change in Haq's sea level curves (>100 m) is generally much larger than the estimates of the other studies (Figure 7). The average difference between high sea level and low sea level during the Mesozoic (Haq, 2014, 2018a, b) and Cenozoic (Haq and Ogg, 2024) is ~80 m. Peak to trough variability during the Paleozoic is somewhat reduced to ~65 m (Haq and Schutter, 2008). This range in sea level variation is comparable to our estimates for icehouse worlds but is much larger than our predictions for greenhouse intervals.

Because underlying data in the Haq et al. studies is not readily available, we cannot reproduce these curves and evaluate how uncertainties in stratigraphic and sedimentological uncertainties are resolved. Theoretically, a stack of eustatic effects driven by aquifer recharge cycles, the emplacement of oceanic Large Igneous Provinces, and thermal expansion of ocean water (Conrad, 2013; Haq and Cloetingh, 2025; Simmons et al., 2020; Wagreich et al., 2014), or modulation by grand orbital cycles (Boulila, 2019; Dutkiewicz et al., 2024; Martinez and Dera, 2015; Zhang et al., 2024) could generate the amplitudes of short term variability alike the reconstructions by Haq and colleagues. However, these factors are unlikely to conspire across large periods of geological history. We can only surmise that their estimates of sea level amplitudes are generally too large for non-glacial periods, as shown previously (Davies and Simmons, 2024; Markwick and Rowley, 1998; Miller et al., 2024) and until the underlying data are made available, their validity cannot be assessed. It should be emphasised that the long-term Tectono-Glacio-Eustatic curve (van der Meer et al., 2022), and the short-term orbital scale glacio-eustatic variability derived here, do not include these additional factors (beyond tectonic and glacio-eustasy), with amplitudes between 10-100 m. It remains to be seen whether additional factors that have eustatic amplitudes of ~100 m, can be discovered.

Several avenues for future improvements exist. In our current approach, we have estimated variability based on a limited set of parameters and have generally assumed linearity i.e. global average temperature to latitude. Non-linear approaches, applied firstly to the long-term paleo-ice-latitude and glacio-eustatic calculations, and secondly to short term variability, would be of great value to explore. Non-linear approaches would need decisions on the shape of non-linearity, and this is however not trivial. Experiments with multiple types of non-linear approaches, dependent on continent configuration, orogeny and ocean-atmosphere circulation, for example using available climate model output for the Phanerozoic, would be of value. In addition, error analyses through for example Monte Carlo based assessment may provide a more statistical way to determine error margins of long term and short term variability. We hope that our initial assessment of temperature, ice and eustatic variability throughout the Phanerozoic presented here, will encourage more detailed analyses in subsequent studies.

## 3. Conclusions

Overall, our analysis has quantified the range of Phanerozoic glacio-eustatic variability utilizing paleogeographic and long-term ice volume reconstructions combined with inferred maximum orbital-scale

variability in global temperature and ice volumes. With this novel methodology we find that short-term, orbital-scale ($10^3$-$10^5$ years) glacio-eustasy was large (~100 m) during the three major Phanerozoic icehouse periods and small (10's of meters) to absent during greenhouse periods. At first order, our results are similar to, and corroborated by, stratigraphic studies that cover shorter time periods. Our continuous Phanerozoic reconstruction of the maximum variability in temperatures, ice volumes and eustasy, may be used as independent constraints and provide important insights into the paleoclimatologic, paleogeographic, paleobiologic development of the Earth System.

## CRediT authorship contribution statement

**Douwe G. van der Meer:** Writing – review & editing, Writing – original draft, Visualization, Validation, Supervision, Software, Resources, Methodology, Investigation, Formal analysis, Data curation, Conceptualization. **Lennert B. Stap:** Writing – review & editing, Validation, Data curation. **Christopher R. Scotese:** Writing – review & editing, Data curation. **Benjamin J.W. Mills:** Writing – review & editing, Data curation. **Appy Sluijs:** Writing – review & editing. **Douwe J.J. van Hinsbergen:** Writing – review & editing.

## Declaration of competing interest

The authors declare the following financial interests/personal relationships which may be considered as potential competing interests: Appy Sluijs reports financial support was provided by European Research Council. Benjamin Mills reports financial support was provided by UK Research and Innovation Natural Environment Research Council. Lennert Stap reports financial support was provided by Dutch Research Council (NWO). If there are other authors, they declare that they have no known competing financial interests or personal relationships that could have appeared to influence the work reported in this paper.

## Acknowledgments

DvdM would like to thank Liz Chiu, David Ray, Roderik van de Wal, and anonymous reviewers for helpful comments on earlier versions of the manuscript. AS thanks the European Research Council for Consolidator Grant 771497. BJWM is funded by the UK Natural Environment Research Council (NE/S009663/1). LBS was funded by the Dutch Research Council (NWO) through VENI grant VI.Veni.202.031.

## Supplementary materials

Supplementary material associated with this article can be found, in the online version, at doi:10.1016/j.epsl.2025.119526.

## Data availability

Data will be made available on request.

## References

Alley, N.F., Hore, S.B., Frakes, L.A., 2020. Glaciations at high-latitude Southern Australia during the early Cretaceous. Austral. J. Earth Sci. 67, 1045–1095. https://doi.org/10.1080/08120099.2019.1590457.

Babcock, L.E., Peng, S.-C., Brett, C.E., Zhu, M.-Y., Ahlberg, P., Bevis, M., Robison, R.A., 2015. Global climate, sea level cycles, and biotic events in the Cambrian period. Palaeoworld, geologic and biotic events and their relationships during the early to Middle Paleozoic 24, 5–15. https://doi.org/10.1016/j.palwor.2015.03.005.

Barker, P.F., Diekmann, B., Escutia, C., 2007. Onset of cenozoic antarctic glaciation. Deep Sea Res. Part II 54, 2293–2307. https://doi.org/10.1016/j.dsr2.2007.07.027.

Boucot, A.J., Xu, C., Scotese, C.R., Morley, R.J., 2013. Phanerozoic Paleoclimate: an atlas of lithologic indicators of climate. https://doi.org/10.2110/sepmcsp.11.

Boulila, S., 2019. Coupling between grand cycles and events in Earth's climate during the past 115 million years. Sci. Rep. 9, 327. https://doi.org/10.1038/s41598-018-36509-7.

Browning, J.V., Miller, K.G., Pak, D.K., 1996. Global implications of lower to middle eocene sequence boundaries on the New Jersey coastal plain: the icehouse cometh. Geology 24, 639–642. https://doi.org/10.1130/0091-7613(1996)024<0639:GIOLTM>2.3.CO;2.

Burgess, P.M., Prince, G.D., 2015. Non-unique stratal geometries: implications for sequence stratigraphic interpretations. Basin. Res. 27, 351–365. https://doi.org/10.1111/bre.12082.

Calvo González, D., Beauchamp, B., Henderson, C.M., 2022. High-frequency sequence stratigraphy of pennsylvanian-lower permian carbonate successions of the Robledo Mountains, New Mexico and the Carnic Alps, Austria: a record of the acme and demise of the late palaeozoic ice age. Facies 69, 2. https://doi.org/10.1007/s10347-022-00658-z.

Clark, P.U., Shakun, J.D., Marcott, S.A., Mix, A.C., Eby, M., Kulp, S., Levermann, A., Milne, G.A., Pfister, P.L., Santer, B.D., Schrag, D.P., Solomon, S., Stocker, T.F., Strauss, B.H., Weaver, A.J., Winkelmann, R., Archer, D., Bard, E., Goldner, A., Lambeck, K., Pierrehumbert, R.T., Plattner, G.-K., 2016. Consequences of twenty-first-century policy for multi-millennial climate and sea-level change. Nature Clim. Change 6, 360–369. https://doi.org/10.1038/nclimate2923.

Conrad, C.P., 2013. The solid Earth's influence on sea level. Geolog. Soc. Am. Bullet. 125, 1027–1052. https://doi.org/10.1130/B30764.1.

Dabard, M.P., Loi, A., Paris, F., Ghienne, J.F., Pistis, M., Vidal, M., 2015. Sea-level curve for the middle to early Late Ordovician in the Armorican Massif (western France): icehouse third-order glacio-eustatic cycles. Palaeogeogr., Palaeoclimatol., Palaeoecol. 436, 96–111. https://doi.org/10.1016/j.palaeo.2015.06.038.

Davies, A., Gréselle, B., Hunter, S.J., Baines, G., Robson, C., Haywood, A.M., Ray, D.C., Simmons, M.D., van Buchem, F.S.P., 2020. Assessing the impact of aquifer-eustasy on short-term cretaceous sea-level. Cretaceous Res. 112, 104445. https://doi.org/10.1016/j.cretres.2020.104445.

Davies, A., Simmons, M.D., 2024. Placing constraints on the nature of short-term eustatic curves. Basin Res. 36, e12832. https://doi.org/10.1111/bre.12832.

De Boer, B., Van de Wal, R.S.W., Bintanja, R., Lourens, L.J., Tuenter, E., 2010. Cenozoic global ice-volume and temperature simulations with 1-D ice-sheet models forced by benthic δ18O records. Annal. Glaciol. 51, 23–33. https://doi.org/10.3189/172756410791392736.

De Vleeschouwer, D., Percival, L.M.E., Wichern, N.M.A., Batenburg, S.J., 2024. Pre-cenozoic cyclostratigraphy and palaeoclimate responses to astronomical forcing. Nat. Rev. Earth Environ. 5, 59–74. https://doi.org/10.1038/s43017-023-00505-x.

Dutkiewicz, A., Boulila, S., Dietmar Müller, R., 2024. Deep-sea hiatus record reveals orbital pacing by 2.4 myr eccentricity grand cycles. Nat. Commun. 15, 1998. https://doi.org/10.1038/s41467-024-46171-5.

Elrick, M., Berkyová, S., Klapper, G., Sharp, Z., Joachimski, M., Frýda, J., 2009. Stratigraphic and oxygen isotope evidence for my-scale glaciation driving eustasy in the early–Middle devonian greenhouse world. Palaeogeogr., Palaeoclimatol., Palaeoecol. 276, 170–181. https://doi.org/10.1016/j.palaeo.2009.03.008.

Fokkema, C.D., Agterhuis, T., Gerritsma, D., de Goeij, M., Liu, X., de Regt, P., Rice, A., Vennema, L., Agnini, C., Bijl, P.K., Frieling, J., Huber, M., Peterse, F., Sluijs, A., 2024. Polar amplification of orbital-scale climate variability in the early eocene greenhouse world. Climate Past 20, 1303–1325. https://doi.org/10.5194/cp-20-1303-2024.

Grossman, E.L., Joachimski, M.M., 2022. Ocean temperatures through the Phanerozoic reassessed. Sci. Rep. 12, 8938. https://doi.org/10.1038/s41598-022-11493-1.

Haq, B., Ogg, J., 2024. Retraversing the highs and lows of cenozoic Sea levels. GSAT 34, 4–11. https://doi.org/10.1130/GSATGG593A.1.

Haq, B.U., 2018a. Jurassic Sea-level variations: A reappraisal. GSA Today 4–10. https://doi.org/10.1130/GSATG359A.1.

Haq, B.U., 2018b. Triassic eustatic variations reexamined. GSA Today 28, 4–9. https://doi.org/10.1130/GSATG381A.1.

Haq, B.U., 2014. Cretaceous eustasy revisited. Global Planetary Change 113, 44–58. https://doi.org/10.1016/j.gloplacha.2013.12.007.

Haq, B.U., Al-Qahtani, A.M., 2005. Phanerozoic cycles of sea-level change on the Arabian Platform. GeoArabia 10, 127–160.

Haq, B.U., Cloetingh, S., 2025. Tectonics vs eustasy: the oceanic container and its contents. Earth-Sci. Rev. 267, 105166. https://doi.org/10.1016/j.earscirev.2025.105166.

Haq, B.U., Schutter, S.R., 2008. A chronology of paleozoic sea-level changes. Science 322, 64–68. https://doi.org/10.1126/science.1161648.

Hinnov, L.A., 2013. Cyclostratigraphy and its revolutionizing applications in the earth and planetary sciences. GSA Bullet. 125, 1703–1734. https://doi.org/10.1130/B30934.1.

Husinec, A., Read, J.F., Prtoljan, B., 2022. Middle and Late Jurassic record of sea-level, sequence development, and carbon-isotope fluctuations, Tethyan Adriatic Carbonate Platform. Croatia. Palaeogeogr., Palaeoclimatol., Palaeoecol. 599, 111030. https://doi.org/10.1016/j.palaeo.2022.111030.

Intergovernmental Panel on Climate Change (IPCC), 2023. Climate Change 2021 – The Physical Science Basis: Working Group I Contribution to the Sixth Assessment Report of the Intergovernmental Panel on Climate Change. Cambridge University Press, Cambridge. https://doi.org/10.1017/9781009157896.

Johnson, J.G., Klapper, G., Sandberg, C.A., 1985. Devonian eustatic fluctuations in Euramerica. GSA Bulletin 96, 567–587. https://doi.org/10.1130/0016-7606(1985)96<567:DEFIE>2.0.CO;2.

Johnson, M.E., 2010. Tracking Silurian eustasy: alignment of empirical evidence or pursuit of deductive reasoning? Palaeogeogr., Palaeoclimatol., Palaeoecol., Early Palaeozoic sea level and climate 296, 276–284. https://doi.org/10.1016/j.palaeo.2009.11.024.

Johnson, M.E., Rong, J.-Y., Kershaw, S., 1998. Calibrating silurian eustasy against the erosion and burial of coastal topography, in: Silurian Cycles Linkages of Dynamic

Stratigraphy with Atmospheric, Oceanic, and Tectonic Cycles, Bulletin. New York State Museum, pp. 3–14.
Judd, E.J., Tierney, J.E., Lunt, D.J., Montañez, I.P., Huber, B.T., Wing, S.L., Valdes, P.J., 2024. A 485-million-year history of Earth's surface temperature. Science 385, eadk3705. https://doi.org/10.1126/science.adk3705.
Karlsen, K.S., Domeier, M., Gaina, C., Conrad, C.P., 2020. A tracer-based algorithm for automatic generation of seafloor age grids from plate tectonic reconstructions. Comput. Geosci. 140, 104508. https://doi.org/10.1016/j.cageo.2020.104508.
Kent, D.V., Olsen, P.E., Rasmussen, C., Lepre, C., Mundil, R., Irmis, R.B., Gehrels, G.E., Giesler, D., Geissman, J.W., Parker, W.G., 2018. Empirical evidence for stability of the 405-kiloyear Jupiter–Venus eccentricity cycle over hundreds of millions of years. Proceed. Nation. Acad. Sci. 115, 6153–6158. https://doi.org/10.1073/pnas.1800891115.
Kirchner, N., Hutter, K., Jakobsson, M., Gyllencreutz, R., 2011. Capabilities and limitations of numerical ice sheet models: a discussion for Earth-scientists and modelers. Quatern. Sci. Rev. 30, 3691–3704. https://doi.org/10.1016/j.quascirev.2011.09.012.
Köhler, P., Knorr, G., Stap, L.B., Ganopolski, A., de Boer, B., van de Wal, R.S.W., Barker, S., Rüpke, L.H., 2018. The effect of obliquity-driven changes on paleoclimate sensitivity during the late pleistocene. Geophys. Res. Lett. 45, 6661–6671. https://doi.org/10.1029/2018GL077717.
Kominz, M.A., Browning, J.V., Miller, K.G., Sugarman, P.J., Mizintseva, S., Scotese, C.R., 2008. Late cretaceous to miocene sea-level estimates from the New Jersey and Delaware coastal plain coreholes: an error analysis. Basin Res. 20, 211–226. https://doi.org/10.1111/j.1365-2117.2008.00354.x.
Kominz, M.A., Miller, K.G., Browning, J.V., Katz, M.E., Mountain, G.S., 2016. Miocene relative sea level on the New Jersey shallow continental shelf and coastal plain derived from one-dimensional backstripping: A case for both eustasy and epeirogeny. Geosphere 12, 1437–1456. https://doi.org/10.1130/GES01241.1.
Laskar, J., 2020. Chapter 4 - Astrochronology, in: Gradstein, F.M., Ogg, J.G., Schmitz, M. D., Ogg, G.M. (Eds.), Geologic time Scale 2020. Elsevier, pp. 139–158. https://doi.org/10.1016/B978-0-12-824360-2.00004-8.
Loi, A., Ghienne, J.-F., Dabard, M.P., Paris, F., Botquelen, A., Christ, N., Elaouad-Debbaj, Z., Gorini, A., Vidal, M., Videt, B., Destombes, J., 2010. The late ordovician glacio-eustatic record from a high-latitude storm-dominated shelf succession: The Bou Ingarf section (Anti-Atlas, Southern Morocco). Palaeogeogr., Palaeoclimatol., Palaeoecol., Early Palaeozoic sea level and climate 296, 332–358. https://doi.org/10.1016/j.palaeo.2010.01.018.
Marcilly, C.M., Torsvik, T.H., Conrad, C.P., 2022. Global phanerozoic sea levels from paleogeographic flooding maps. Gondwana Res. https://doi.org/10.1016/j.gr.2022.05.011.
Markwick, P.J., Rowley, D.B., 1998. The geological evidence for triassic to pleistocene glaciations: implications for eustasy, in: Pindell, J.L., Drake, C.L. (Eds.), Paleogeographic Evolution and Non-Glacial Eustasy, Northern South America. SEPM Society for Sedimentary Geology, p. 0. https://doi.org/10.2110/pec.98.58.0017.
Martinez, M., Dera, G., 2015. Orbital pacing of carbon fluxes by a ~9-my eccentricity cycle during the Mesozoic. Proceed. Nation. Acad. Sci. 112, 12604–12609. https://doi.org/10.1073/pnas.1419946112.
Miall, A.D., 2010. The Geology of Stratigraphic Sequences. Springer-Verlag, Berlin, Heidelberg.
Milanković, M., 1930. Mathematische Klimalehre und astronomische Theorie der Klimaschwankungen. Gebrüder Borntraeger, Berlin.
Miller, K.G., Schmelz, W.J., Browning, J.V., Rosenthal, Y., Hess, A.V., Kopp, R.E., Wright, J.D., 2024. Global mean and relative sea-level changes over the past 66 myr: implications for early eocene ice sheets. Earth Sci. Syst. Soc. 3, 10091. https://doi.org/10.3389/esss.2023.10091.
Mills, B.J.W., Krause, A.J., Scotese, C.R., Hill, D.J., Shields, G.A., Lenton, T.M., 2019. Modelling the long-term carbon cycle, atmospheric CO2, and Earth surface temperature from late neoproterozoic to present day. Gondwana Res. 67, 172–186. https://doi.org/10.1016/j.gr.2018.12.001.
Mitchell, R.N., Gernon, T.M., Cox, G.M., Nordsvan, A.R., Kirscher, U., Xuan, C., Liu, Y., Liu, X., He, X., 2021. Orbital forcing of ice sheets during snowball Earth. Nat. Commun. 12, 4187. https://doi.org/10.1038/s41467-021-24439-4.
Osman, M.B., Tierney, J.E., Zhu, J., Tardif, R., Hakim, G.J., King, J., Poulsen, C.J., 2021. Globally resolved surface temperatures since the last Glacial maximum. Nature 599, 239–244. https://doi.org/10.1038/s41586-021-03984-4.
Prokoph, A., Shields, G.A., Veizer, J., 2008. Compilation and time-series analysis of a marine carbonate δ18O, δ13C, 87Sr/86Sr and δ34S database through Earth history. Earth Sci. Rev. 87 (3–4), 113–133. https://doi.org/10.1016/j.earscirev.2007.12.003.
Ray, D.C., van Buchem, F.S.P., Baines, G., Davies, A., Gréselle, B., Simmons, M.D., Robson, C., 2019. The magnitude and cause of short-term eustatic cretaceous sea-level change: A synthesis. Earth-Sci. Rev. 197, 102901. https://doi.org/10.1016/j.earscirev.2019.102901.
Rohling, E.J., Foster, G.L., Gernon, T.M., Grant, K.M., Heslop, D., Hibbert, F.D., Roberts, A.P., Yu, J., 2022. Comparison and synthesis of sea-level and deep-sea temperature variations over the past 40 million years. Rev. Geophys. 60. https://doi.org/10.1029/2022RG000775 e2022RG000775.
Rohling, E.J., Rohling, E.J., Sluijs, A., Dijkstra, H.A., Köhler, P., van de Wal, R.S.W., von der Heydt, A.S., Beerling, D.J., Berger, A., Bijl, P.K., Crucifix, M., DeConto, R., Drijfhout, S.S., Fedorov, A., Foster, G.L., Ganopolski, A., Hansen, J., Hönisch, B., Hooghiemstra, H., Huber, M., Huybers, P., Knutti, R., Lea, D.W., Lourens, L.J., Lunt, D., Masson-Delmotte, V., Medina-Elizalde, M., Otto-Bliesner, B., Pagani, M., Pälike, H., Renssen, H., Royer, D.L., Siddall, M., Valdes, P., Zachos, J.C., Zeebe, R.E., 2012. Making sense of palaeoclimate sensitivity. Nature 491, 683–691. https://doi.org/10.1038/nature11574.
Rygel, M.C., Fielding, C.R., Frank, T.D., Birgenheier, L.P., 2008. The magnitude of late paleozoic glacioeustatic fluctuations: a synthesis. J. Sediment. Res. 78, 500–511. https://doi.org/10.2110/jsr.2008.058.
Sahagian, D., Pinous, O., Olferiev, A., Zakharov, V., 1996. Eustatic curve for the middle jurassic—Cretaceous based on Russian platform and Siberian stratigraphy: zonal resolution. AAPG Bullet. 80, 1433–1458. https://doi.org/10.1306/64ED9A56-1724-11D7-8645000102C1865D.
Scotese, C.R., Song, H., Mills, B.J.W., van der Meer, D.G., 2021. Phanerozoic paleotemperatures: the earth's changing climate during the last 540 million years. Earth-Sci. Rev., 103503 https://doi.org/10.1016/j.earscirev.2021.103503.
Scotese, C.R., Vérard, C., Burgener, L., Elling, R.P., Kocsis, A.T., 2024. The cretaceous world: plate tectonics, paleogeography, and paleoclimate. Geolog. Soc. 544. https://doi.org/10.1144/SP544-2024-28. SP544-2024–28.
Scotese, C.R., Wright, N.M., 2018. PALEOMAP paleodigital elevation models (PaleoDEMS) for the phanerozoic PALEOMAP project. http://www.earthbyte.org/paleodem-resource-scotese-and-wright-2018/.
Simmons, M.D., Miller, K.G., Ray, D.C., Davies, A., van Buchem, F.S.P., Gréselle, B., 2020. Chapter 13 - Phanerozoic Eustasy, in: Gradstein, F.M., Ogg, J.G., Schmitz, M. D., Ogg, G.M. (Eds.), Geologic Time Scale 2020. Elsevier, pp. 357–400. https://doi.org/10.1016/B978-0-12-824360-2.00013-9.
Shaviv, N.J., Svensmark, H., Veizer, J., 2023. The Phanerozoic climate. Ann. N.Y. Acad. Sci. 1519 (1), 7–9. https://doi.org/10.1111/nyas.14920.
Song, H., Wignall, P.B., Song, H., Dai, X., Chu, D., 2019. Seawater temperature and dissolved oxygen over the past 500 million years. J. Earth Sci. 30, 236–243. https://doi.org/10.1007/s12583-018-1002-2.
Spasojevic, S., Gurnis, M., 2012. Sea level and vertical motion of continents from dynamic earth models since the Late Cretaceous. AAPG Bullet. 96, 2037–2064. https://doi.org/10.1306/03261211121.
Stap, L.B., van de Wal, R.S.W., de Boer, B., Bintanja, R., Lourens, L.J., 2017. The influence of ice sheets on temperature during the past 38 million years inferred from a one-dimensional ice sheet–climate model. Climate Past 13, 1243–1257. https://doi.org/10.5194/cp-13-1243-2017.
Vail, P.R., Mitchum, R.M., Thompson, S.I., 1977. Seismic stratigraphy and global changes of sea level: part 4. Global Cycles Relat. Chang. Sea Level 165, 83–97.
Valdes, P.J., Scotese, C.R., Lunt, D.J., 2021. Deep ocean temperatures through time. Climate Past 17, 1483–1506. https://doi.org/10.5194/cp-17-1483-2021.
van der Meer, D.G., Scotese, C.R., Mills, B.J.W., Sluijs, A., van den Berg van Saparoea, A.-P., van de Weg, R.M.B., 2022. Long-term phanerozoic global mean sea level: insights from strontium isotope variations and estimates of continental glaciation. Gondwana Res. 111, 103–121. https://doi.org/10.1016/j.gr.2022.07.014.
van der Meer, D.G., van den Berg van Saparoea, A.P.H., van Hinsbergen, D.J.J., van de Weg, R.M.B., Godderis, Y., Le Hir, G., Donnadieu, Y., 2017. Reconstructing first-order changes in sea level during the Phanerozoic and Neoproterozoic using strontium isotopes. Gondwana Res. 44, 22–34. https://doi.org/10.1016/j.gr.2016.11.002.
van Hinsbergen, D.J.J., Abels, H.A., Bosch, W., Boekhout, F., Kitchka, A., Hamers, M., van der Meer, D.G., Geluk, M., Stephenson, R.A., 2015. Sedimentary geology of the middle carboniferous of the Donbas region (Dnieprr-Donets basin, Ukraine). Sci. Rep. 9099. https://doi.org/10.1038/srep09099, 5.
Vérard, C., Hochard, C., Baumgartner, P.O., Stampfli, G.M., 2015. 3D palaeogeographic reconstructions of the phanerozoic versus sea-level and Sr-ratio variations. J. Paleogeogr. 4, 64–84. https://doi.org/10.3724/SP.J.1261.2015.00068.
Wagreich, M., Lein, R., Sames, B., 2014. Eustasy, its controlling factors, and the limno-eustatic hypothesis – concepts inspired by Eduard Suess. Austr. J. Earth Sci. 107, 115–131.
Westerhold, T., Marwan, N., Drury, A.J., Liebrand, D., Agnini, C., Anagnostou, E., Barnet, J.S.K., Bohaty, S.M., De Vleeschouwer, D., Florindo, F., Frederichs, T., Hodell, D.A., Holbourn, A.E., Kroon, D., Lauretano, V., Littler, K., Lourens, L.J., Lyle, M., Pälike, H., Röhl, U., Tian, J., Wilkens, R.H., Wilson, P.A., Zachos, J.C., 2020. An astronomically dated record of Earth's climate and its predictability over the last 66 million years. Science 369, 1383–1387. https://doi.org/10.1126/science.aba6853.
Wright, J.K., 2025. Review of Oxfordian (Upper Jurassic) sequence stratigraphy of England (Yorkshire to Dorset) and a comparison with the North Sea Basin. In: Proceedings of the Geologists' Association 101125. https://doi.org/10.1016/j.pgeola.2025.101125.
Wright, N.M., Seton, M., Williams, S.E., Whittaker, J.M., Müller, R.D., 2020. Sea-level fluctuations driven by changes in global ocean basin volume following supercontinent break-up. Earth-Sci. Rev. 208, 103293. https://doi.org/10.1016/j.earscirev.2020.103293.
Young, A., Flament, N., Williams, S.E., Merdith, A., Cao, X., Dietmar Müller, R., 2022. Long-term phanerozoic sea level change from solid Earth processes. Earth Planet. Sci. Lett. 584, 117451. https://doi.org/10.1016/j.epsl.2022.117451.
Zachos, J.C., Dickens, G.R., Zeebe, R.E., 2008. An early cenozoic perspective on greenhouse warming and carbon-cycle dynamics. Nature 451, 279–283. https://doi.org/10.1038/nature06588.
Zhang, Y., Fang, Q., Wu, H., Zeeden, C., Cui, Y., Shi, M., Zhang, S., Yang, T., Li, H., 2024. Changes in $pCO2$ and climate paced by grand orbital cycles in the late Cenozoic. Global Planet. Change 239, 104493. https://doi.org/10.1016/j.gloplacha.2024.104493.